Microfluid Nanofluid (2017) 21:63
DOI 10.1007/s10404-017-1898-3

RESEARCH PAPER

Highly integrated polymeric microliquid flow controller for droplet microfluidics

J. Etxebarria[1,2] · J. Berganzo[1] · M. Brivio[3] · H. Gardeniers[4] · A. Ezkerra[1]

Received: 9 December 2016 / Accepted: 8 March 2017 / Published online: 18 March 2017

Abstract Microfluidic applications demand accurate control and measurement of small fluid flows and volumes, and the majority of approaches found in the literature involve materials and fabrication methods not suitable for a monolithic integration of different microcomponents needed to make a complex Lab-on-a-Chip (LoC) system. The present work leads to a design and manufacturing approach for problem-free monolithic integration of components on thermoplastics, allowing the production of excellent quality devices either as stand-alone components or combined in a complex structures. In particular, a polymeric liquid flow controlling system (LFCS) at microscale is presented, which is composed of a pneumatic microvalve and an on-chip microflow sensor. It enables flow regulation between 30 and 230 μl/min with excellent reproducibility and accuracy (error lower than 5%). The device is made of a single Cyclic Olefin Polymer (COP) piece, where the channels and cavities are hot-embossed, sealed with a single COP membrane by solvent bonding and metalized, after sealing, to render a fully functional microfluidic control system that features on-chip flow sensing. In contrast with commercially available flow control systems, the device can be used for high-quality flow modulation in disposable LoC devices, since the microfluidic chip is low cost and replaceable from the external electronic and pneumatic actuators box. Functionality of the LFCS is tested by connecting it to a microfluidic droplet generator, rendering highly stable flow rates and allowing generation of monodisperse droplets over a wide range of flow rates. The results indicate the successful performance of the LFCS with significant improvements over existing LFCS devices, facing the possibility of using the system for biological applications such as generating distinct perfusion modes in cell culture, novel digital microfluidics. Moreover, the integration capabilities and the reproducible fabrication method enable straightforward transition from prototype to product in a way that is lean, cost-effective and with reduced risk.

Keywords Microflow control · Monolithic · Polymer · Droplet microfluidics

1 Introduction

Handling of small flow rates is becoming increasingly crucial for diverse economically important applications, as accurate flow control is finding new niches in the oil refining, analytical instrumentation, food and pharma industries. Point-of-care (POC) devices in medicine, microbioreactors in biotechnology, massive parallelization of chemical microfactories or condition monitoring of hydraulic systems in automotive industry are some of the success cases where accurate and repeatable mass flow control is required. In LoC or POC systems, the precise flow control is of utmost importance in order to eliminate dispensing, dosing or dilutions errors and thus obtain satisfactory results in diagnosis or biological protocols.

Regarding microscale, there is a wealth of miniaturized liquid flow controlling system (LFCS) devices in the

✉ J. Etxebarria
jetxebarria002@gmail.com

[1] Microsystems Department, IK4-IKERLAN, Arrasate-Mondragón, Spain

[2] BIOMICs Research Group- Microfluidics Cluster, EHU/UPV University of Basque Country, Vitoria-Gasteiz, Spain

[3] Micronit Microfluidics B.V., Enschede, The Netherlands

[4] Mesoscale Chemical Systems (MCS) MESA+ Institute for Nanotechnology, Enschede, The Netherlands

literature (Lammerink et al. 1993; Xie et al. 2003; Xu et al. 2010) that set, measure and control the particular flow of a gas or a liquid, and the trend leads towards modular systems that can be easily constructed by assembling different parts. However, in the literature there is still lack of a microflow controller that allows a satisfactory performance and that is easy to fabricate, cost-effective, can be adequately integrated in full polymeric and monolithic LoCs without dimensional or assembly errors and is compatible with industrial mass-production techniques (Kohl et al. 2004).

In this work, two modular components have been integrated into a monolithic closed-loop liquid flow-regulating system fully made of Cyclic Olefin Polymer (COP). The device is obtained by hot embossing the structures in COP and sealing them with a COP membrane and is composed of (1) a channel with a post-produced on-chip calorimetric flow sensor in bypass configuration, which is patterned in nickel and features precise and reproducible flow rate measurements over a wide range at low heater temperature and (2) a flow-regulating pneumatic membrane microvalve that shows tunable and highly repetitive flow regulation capabilities. The LFCS has proven excellent reproducibility and accuracy while allowing highly stable flows, which is demanded in plenty of applications such as droplet microfluidics. Therefore, the functionality of the LFCS has been tested in high-throughput hexadecane (HD) in water (W) droplet generation, enabling a stable system and successful monodisperse droplet generation for a wide flow range. The satisfactory results demonstrate that the LFCS perfectly matches the response of commercially available systems that are costly and difficult to integrate and meets all the requirements to be effectively used in realistic scenarios of plenty of applications.

2 Device architecture and working principle

2.1 LFCS architecture and working principle

Every flow controlling system is composed of two elements, the flow metre and the regulating valve. The microvalve module can be actuated in order to tune the amount of liquid passing through a microfluidic chip, and the microflow sensor can be employed to measure the precise flow rate at each moment. Thus, by combining both components with electronics for closed-loop control, the valve can be regulated according to the readouts of the sensor to deliver the desired amount of liquid.

The present LFCS is fully integrated by hot embossing in a thermoplastic material, COP, and a finished device is shown in Fig. 1a. It is composed of two monolithically integrated modular components, a flow-regulating pneumatic microvalve and a post-produced on-chip calorimetric thermal flow sensor in a bypass configuration for high flow rates. These two components have been successfully demonstrated in previous works as stand-alone components (Etxebarria et al. 2014, 2016).

The microvalve works by deflecting the active COP membrane (Fig. 1b olive colour) towards the valve seat (Fig. 1b green colour) as a result of an externally applied pressure and regulates the flow by reducing the fluidic section and consequently increasing the fluidic resistance in the valve and decreasing the flow rate. By controlling the applied pressure, a partial or total blocking of the flow is achieved, which effectively describes the principle of flow modulation (Etxebarria et al. 2014). A microvalve with a membrane diameter of 3 mm and an actuating membrane of 100 µm, a seat diameter of 1 mm and a gap of 20 µm, was chosen from a previous characterization for an array of 18 microvalve designs. This construction was considered the best option for control since it features a linear flow regulation profile that facilitates flow regulation and an affordable closing pressure of 2 bar (Etxebarria Elezgarai 2015).

The calorimetric sensor consists of a central heater surrounded by two temperature sensors, placed at an equal distance upstream and downstream, with the Ni strips sputtered directly on a finalized microfluidic channel. When the sensor operates at constant heater voltage, the heat generated by the heater is mostly dissipated by conduction in the COP membrane and by forced convection due to the liquid that flows through the microchannel, creating a temperature distribution at the membrane that is characteristic of that particular flow rate. This temperature distribution causes a difference in resistance at the sensors, which can be directly measured as a voltage signal. The optimum sensor configuration was obtained from an array of 16 designs, taking the dimensions of the meanders (width and length of the heater and sensors), as well as the distance between the heater and sensing elements as variables. The best ratio of output signal to flow rate was obtained for Design D12, for a heater operating at 50 °C, 2.5 mm long, 20 µm thick and sensors 2 mm long and 20 µm thick, with a distance between the elements of 60 µm. This configuration provides the highest sensitivity by maximizing heat transfer to the fluid and sensing area and minimizing cross-talk between sensors (Etxebarria et al. 2016). The flow sensor requires a bypass construction to widen its detection range and thus match with the flow range that the microvalve can regulate. The bypass consists of a sensing channel 80 µm high and 500 µm wide and a bypass channel 250 µm high and 2 mm wide, with a 100-µm sealing membrane.

The working principle of the LFCS is depicted in Fig. 2. First, a constant-pressure drop is used to drive the liquid through the device. The resulting flow rate is measured by the sensor (FT), which communicates the signal to the pressure regulator (PR) that controls the membrane via a computer-aided PID control (LabVIEW). The closed loop compares the signal against the

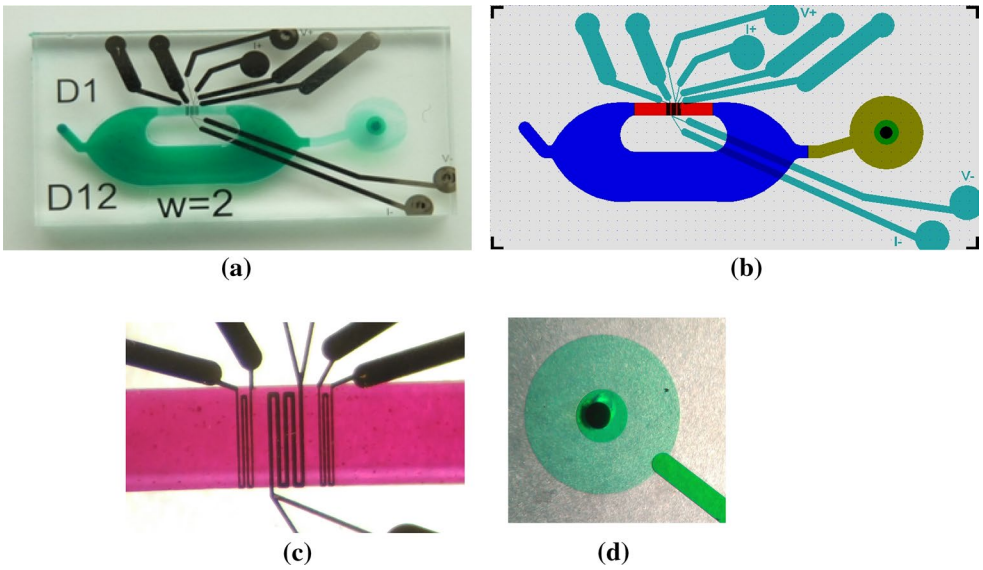

Fig. 1 Architecture of the microfluidic flow controller. **a** Image of a finished device in a 2 cm^2 dye filled with diluted *green-coloured* solution. **b** Layout of the device where each colour refers to a different functional part. *Olive colour* represents the active movable COP membrane that deflects when an external force is applied to regulate the flow rate passing through the microfluidic chip, the *green colour* illustrates the valve seat where the membrane collapses and closes the microvalve when sufficient pressure is applied, and the *black colour* shows the outlet for the liquid. *Red colour* refers to a flow sensing channel, *turquoise colour* representing a calorimetric flow sensing strips patterned in nickel and outside of the covering membrane, and *blue colour* shows the bypass channel required to widen the measuring range. The on-chip sensor detects the asymmetric thermal profile around the central heater caused by forced convection due to the flowing fluid in the microchannel, and measures the temperature difference upstream and downstream sensors as a voltage signal. **c** Close-up image of the Ni microsensor consisting of a central heater 2.5 mm long and 20 µm wide and surrounding temperature sensors 2 mm long and 20 µm wide, the distance between elements being 60 µm. **d** Close-up image of a finished microvalve filled with a *green-coloured* solution, which highlights the different parts of the structure, being the membrane diameter 3 mm, actuating membrane 100 µm, seat diameter 1 mm, and membrane gap 20 µm. Further information on single component architecture and working principle is addressed in previous publications (Etxebarria et al. 2014, 2016)

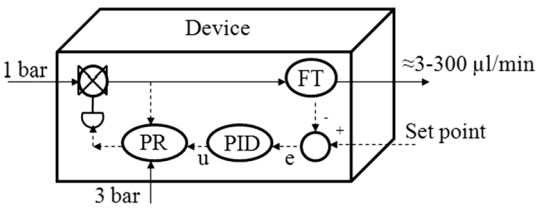

Fig. 2 Block diagram of the LFCS working principle, where the flow sensor (FT) sends the flow rate value to the PID controller, which modulates the pressure (PR) on the valve (⊗) to minimize the error (e±) between the measured flow rate and the set point defined by the user

set point defined by the user and modulates the pressure on the membrane to arrive at the desired flow rate.

2.2 Droplet generator architecture and working principle

In recent years, droplet-based microfluidics is emerging for the study of cells, since accurate medium composition control and enhanced mixing due to internal recirculation can be easily achieved using droplets, in which cells can be encapsulated with different mediums at different concentrations, allowing chemical gradients of medium and nutrients (Choi et al. 2012).

Microfluidic droplet generators work by combining immiscible fluids and generating a shear force on the continuous phase causing it to break up into discrete droplets. Critical factors for the drop formation include the materials chosen for the device, the fluids used for droplet formation, the size of the nozzle restriction, the viscosity of the immiscible phases, the use of surfactants and also the dimensionless capillary number, C_a, since the type of the flow depends on it and above a critical capillary value, which is system dependent, droplet formation starts (Pollack et al. 2002; Teh et al. 2008; Utada et al. 2005).

The surface wettability of the channel is critical to form aqueous-in-organic (W/O) or organic-in-aqueous (O/W) droplets. To prevent organic droplets to stick on channel walls, hydrophilic channels are required (e.g. untreated glass) and for water droplets hydrophobic channels are needed (e.g. coated glass). Moreover, surfactants are usually used to alter the channel surface wettability and prevent coalescence of the droplets.

An equilibration time is necessary to obtain droplets that are stable in size, and the stabilization depends on the nature of the imposed flow rates or the materials used in the whole system, since depending on the elasticity of the fluidic system (syringe, tube, device) and their deformability under pressure changes the stabilization time may vary considerably (Bertholle and Velvé Casquillas). Regarding the nature of the fluids flow, the most common instruments to supply flow rate of fluids are the syringe pumps and the pressure-driven pumps. The syringe pumps are widely used as the flow rates can be easily controlled by setting the rotation speed of the pump motor, and precise flow rate control and good reproducibility of the assays can be achieved at high flow rates. However, comparing the dynamic characteristics of both systems, the main drawback for syringe pumps is that the step motor produces periodic vibrations in the rotary screw that are transmitted to the syringe piston translation, generating periodic variations of the flow rate and increasing the stabilization time. Syringe pumps also show poor responsiveness at low flow rates, allow a limited amount of fluid and are incompatible with valve-based closed systems. On the contrary, pressure-driven flows shift almost instantaneously, showing a fast response time for a large range of flow rates, and do not generate vibrations and periodic fluctuations since pressure is regulated through a pressure controller. The amount of dispense fluid is not limited to a few millilitres as for the syringes and can vary up to several litres with the same performances (Zenget al. 2015). Therefore, the current experience points that pressure-driven flow generation systems are more appropriate to control droplet generation systems.

Droplet formation is tested in a single-junction droplet generator device provided by Micronit Microfluidics, which posses a channel of 100 µm width and 20 µm high and relies on a highly precise 10-µm restriction in a flow-focused configuration. The microfluidic channels are structured in 1.1-mm glass layer, and a 700-µm glass layer with holes is bonded on top of it, enclosing the channels and providing the microfluidic ports. The flow-focused droplet generator (FFDG) is depicted in Fig. 3a, b, and the droplets created ahead of the restriction for a flow-focused configuration can be seen in Fig. 4.

3 Materials and methods

3.1 Fabrication of the LFCS

The LFCS is fabricated at wafer level using a COP as a substrate material. In short, the general method consists in (1) replicating the valve and the sensor structures by hot embossing, (2) sealing these structures with a COP membrane by a solvent bonding that ensures a smooth surface and (3) metal deposition on top of the covering membrane (Etxebarria et al. 2014, 2016).

For the hot embossing process, a master mould made of SU8 and a COP substrate wafer are heated above the glass transition temperature of the polymer, 157 °C; both parts are brought together and pressed applying the embossing force under vacuum, 7.5 kN. After the required embossing time, 80 min, both parts are cooled down and separated at demoulding temperature, T_d, where the sensor and bypass channels and the microvalve cavities are obtained. Then, the inlet/outlet ports are drilled for fluidic connection, and the structures are covered with a flat 100-µm COP membrane to finalize the fluidic part, using a solvent bonding method and chlorobenzene as a solvent. The sealing procedure involves spinning 4 ml of chlorobenzene on top of the membrane to obtain an adhering membrane surface which is brought into contact with the patterned substrate and pressed against it. The solvent traces are removed by degassing the finalized device under vacuum (Etxebarria et al. 2014). Finally, the external thermal flow sensor is patterned by sputtering Ni resistors on the outside of the finalized device. The process starts by cleaning the surface of the finalized device with oxygen plasma treatment for 2 min at 90 W. Next, OIR-positive photo-resist is spin-coated and soft-baked under IR for 12 min at 95 W. The resist is exposed to a UV dose of 350 mJ cm^{-2} to define the sensor elements, developed in a bath of positive resist developer and rinsed with DIW. Prior to Ni sputtering, the wafer is again cleaned with oxygen plasma for 2 min at 90 W. Next, a layer of 100 nm of Ni is deposited and a lift-off performed (Etxebarria et al. 2016). The LFCS devices

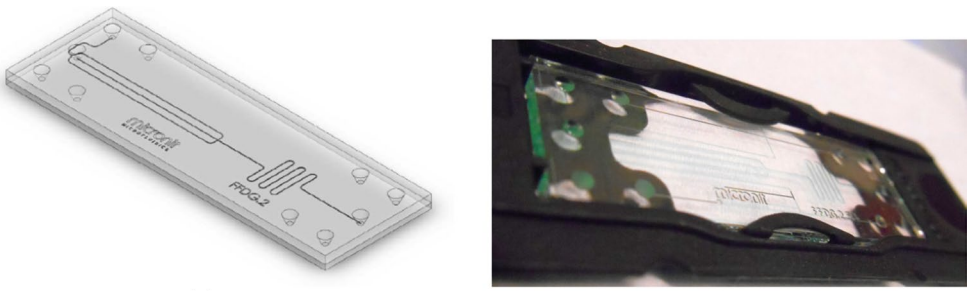

(a) (b)

Fig. 3 Focused-flow droplet generator chip from Micronit Microfluidics. **a** Scheme and **b** finalized chip of single-junction FFDG with a channel width and depth of 100 and 20 µm, respectively, and a restriction nozzle of 10 µm

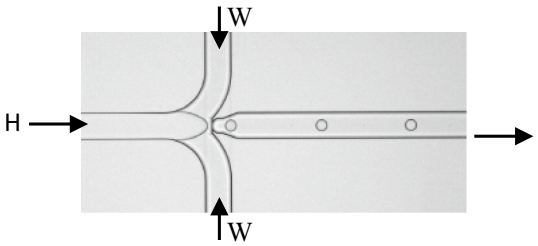

Fig. 4 Hexadecane in water (O/W) droplet formation in a focused-flow droplet generator. The sheet flow is created ahead of the 10-µm restriction

are finalized by dicing the COP wafer. This fabrication method assures repetitive batch-to-batch results and is compatible with industrial manufacturing techniques, such as injection moulding, roll-to-roll bonding and inkjet printing techniques, paving the way for mass production of a variety of integrated components and such as the presented flow controller.

4 Characterization and results

4.1 Characterization of the LFCS

In order to characterize the LFCS, the device has been fitted in a packaging, Fig. 5, which provides fluidic connection to the device, pneumatic actuation to the valve and powering and readout connections to the sensor by means of a mounted electronic PCB.

The characterization set-up consists of the aforementioned packaging, a pressure dispenser for moving the fluids (Ultra® 1400 EFD), a miniature pressure regulator to modulate the pressure on the membrane (Parker Hannifin S.L.), a data logger for data acquisition (Agilent 34970, Agilent technologies), an electronic PCB dedicated to driving of the LFCS operation and a computer-aided PID control loop feedback mechanism, programmed in LabVIEW. The actual set-up and its block diagram are shown in Fig. 6a, c, respectively.

The device is characterized by analysing the match between a flow rate routine defined by the user and the one delivered by the LFCS. For this, a flow rate routine of increasing steps of 10 µl/min is defined and the routine is performed three times. The characterization results in Fig. 7 show the flow rate delivered by the LFCS in comparison with the one fixed as a set point and the one measured by a commercial flow sensor. The results show excellent accuracy and reproducibility, with an error of less than 5% in the range between 30 and 230 µl/min, less than 15% below 30 µl/ and around 30% for the stopped liquid.

4.2 Validation of the LFCS in a droplet generation system

Correct performance of droplet-based microfluidics demands highly stable flows in order to acquire a homogeneous droplet size with proper generation speed (or frequency), since steady flows avoid oscillations of pressure inside the system that can break its steady state. Therefore, droplet microfluidics is used to effectively prove the functionality of the LFCS in a realistic scenario, where the device is used to control the continuous water phase (W) in high-throughput flow-focused hexadecane (HD) in water (W) droplet formation, by connecting the LFCS device to the glass droplet generator.

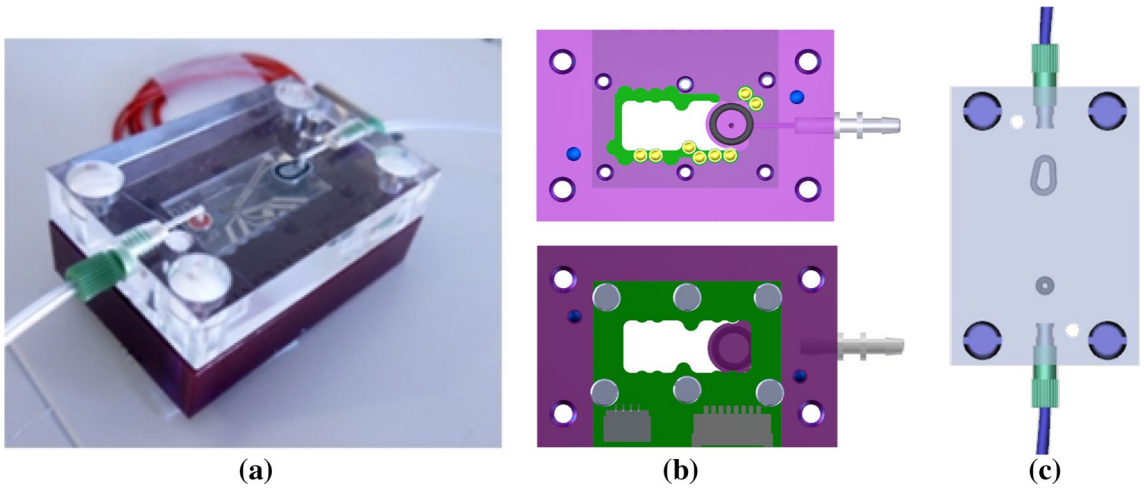

Fig. 5 **a** Image of the packaging with a LFCS device, which provides **b** connection for pneumatic actuation to the valve and powering and readout connections to the sensor by means of a mounted electronic PCB and **c** upchurch connector with tubing for fluidic connection to the device

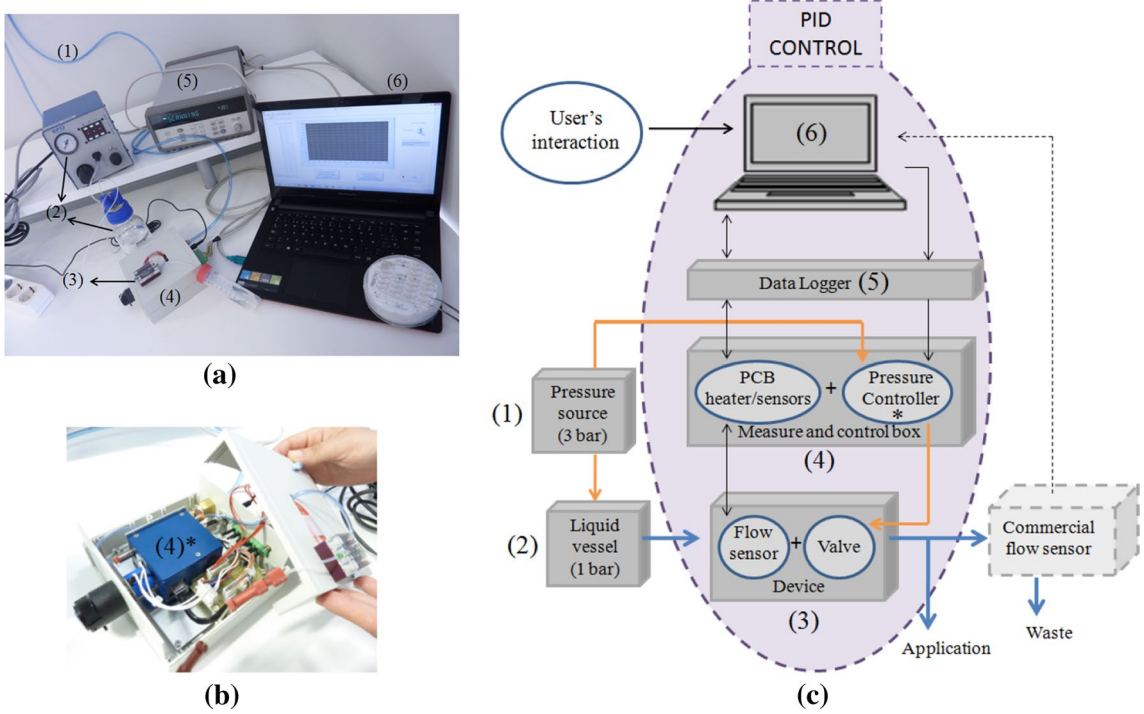

Fig. 6 **a** Set-up for characterization of the LFCS consisting of (1) a main pressure source (3–6 bar), (2) a pressure dispenser for moving the fluids (Ultra® 1400 EFD) and a liquid vessel, (3) a flow controlling device, (4) measure and control box with a pressure regulator (Parker Hannifin S.L) to modulate the pressure on the membrane and connections for PID control, (5) a data logger for data acquisition (Agilent 34970A Agilent technologies) and (6) a LabVIEW-based control program; **b** measure and control box that features a pressure controller to regulate the actuation on the valve membrane and a PCB that integrates all control elements and connects them to the PID controller; **c** block diagram of the experimental set-up. The *orange rows* refer to compressed air, *black rows* refer to electrical signal (input information or execution commands), and the *blue rows* refer to the liquid flow, whose flow rate is measured before ending in the waste. The user options include desired flow rate, working temperature of the sensor and zero-flow signal balance

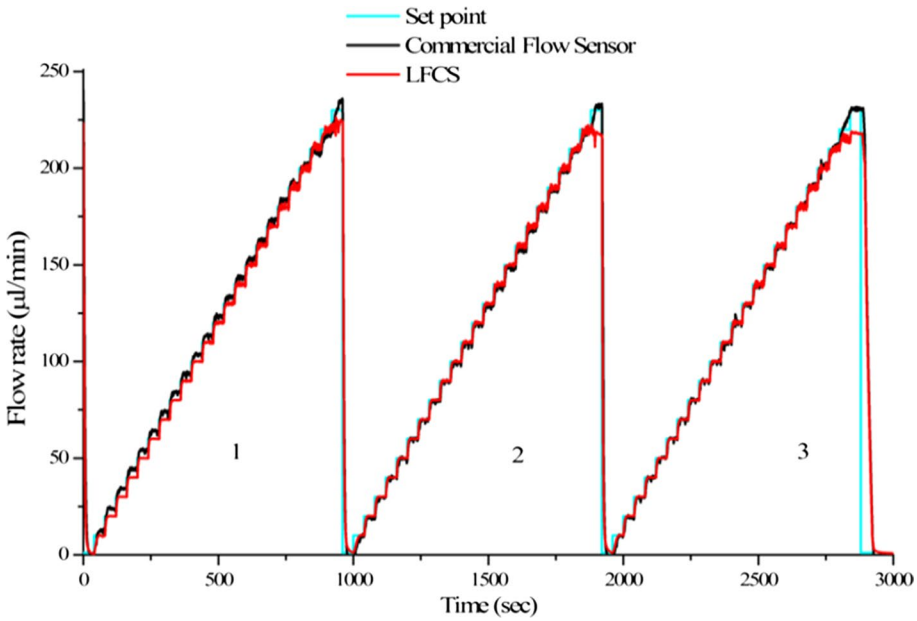

Fig. 7 Characterization of the LFCS with three cycles of increasing 10 µl/min steps and comparison against a commercial flow sensor

The set-up for the droplet generation comprises a packaging (Micronit Microfluidics B.V.) to provide fluidic connection for water and hexadecane to the FFDG device (Fig. 8a), the LFCS device previously detailed to precisely control the water flow rate, a syringe pump (Harvard PHD 2000) to accurately fix the hexadecane flow rate in a steady state, and a Leica DMI 5000 M inverted microscope with a MotionBLITZ EoSens®mini2 high-speed camera for recording the droplets in the FFDG device. The block diagram and the set-up for the experiments can be seen in Fig. 8b, c.

The formation of hexadecane (O) droplets in water (W) is realized by maintaining the hexadecane flow rate (Q_{HD}) constant and varying the water flow rate (Q_W) in which 2% Tween80 (v/v) is added so as to avoid merging of HD droplets. The main reason of maintaining Q_{HD} constant is that this fluid is controlled by a syringe pump and thus more equilibration time is required to stabilize the system (Zeng et al. 2015). In consequence, the stabilization times of 30 and 5 min have been used for Q_{HD} and Q_W, respectively.

In Fig. 9a the diameters of the generated droplet measured inside the channel (D_c) are depicted. Droplets with D_c diameters between 20 and 75 μm (diameters outside the channel being between 25 and 55 μm) were generated depending on the flow rate of HD and W phases. Figure 9b, c shows the images obtained during the formation of droplets being the direction of the flow from right to left, and since the channel height is 20 μm, the droplets inside the channel appear as flattened spheres. The generated droplets were collected on a reservoir in order to analyse their stability, and no droplet merging problem was observed, as can be seen in Fig. 9c.

Results show that when the organic phase and aqueous phase flow rates ratio (Q_{HD}/Q_W) is too high, the droplets

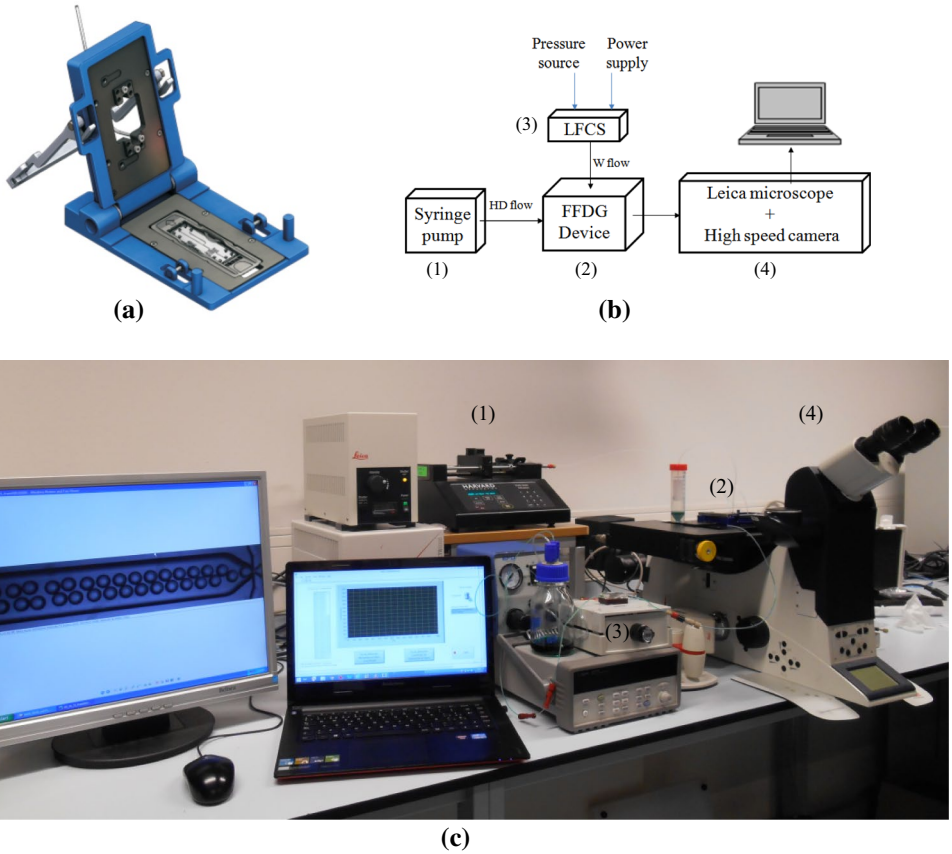

Fig. 8 Set-up employed for droplet generation experiments. **a** Packaging, provided by Micronit, used to adequately connect the fluidic tubings to the flow-focused droplet generator. The *bottom* part possesses the chip holder and the *top* part brings the fluidic connections to the circuit; **b** block diagram of the set-up employed for hexadecane in water droplet generation (O/W). The aqueous phase is controlled with the LFCS and the organic phase with a syringe micropump employing sufficiently high HD speeds to ensure pulse-free steady velocities. The droplets are formed within the droplet generator device with a focused-flow configuration and are recorded with a high-speed camera mounted on an inverted Leica microscope; **c** set-up used for the high-throughput hexadecane in water droplet generation that comprises (1) a syringe pump to accurately fix the hexadecane flow rate in a steady state (Harvard PHD 2000) (2) a packaging to provide fluidic connections to the FFDG device, (3) the LFCS to precisely control the water flow rate, and (4) a Leica DMI 5000 M inverted microscope with a MotionBLITZ EoSens®mini2 high-speed camera for recording the droplets in the FFDG device

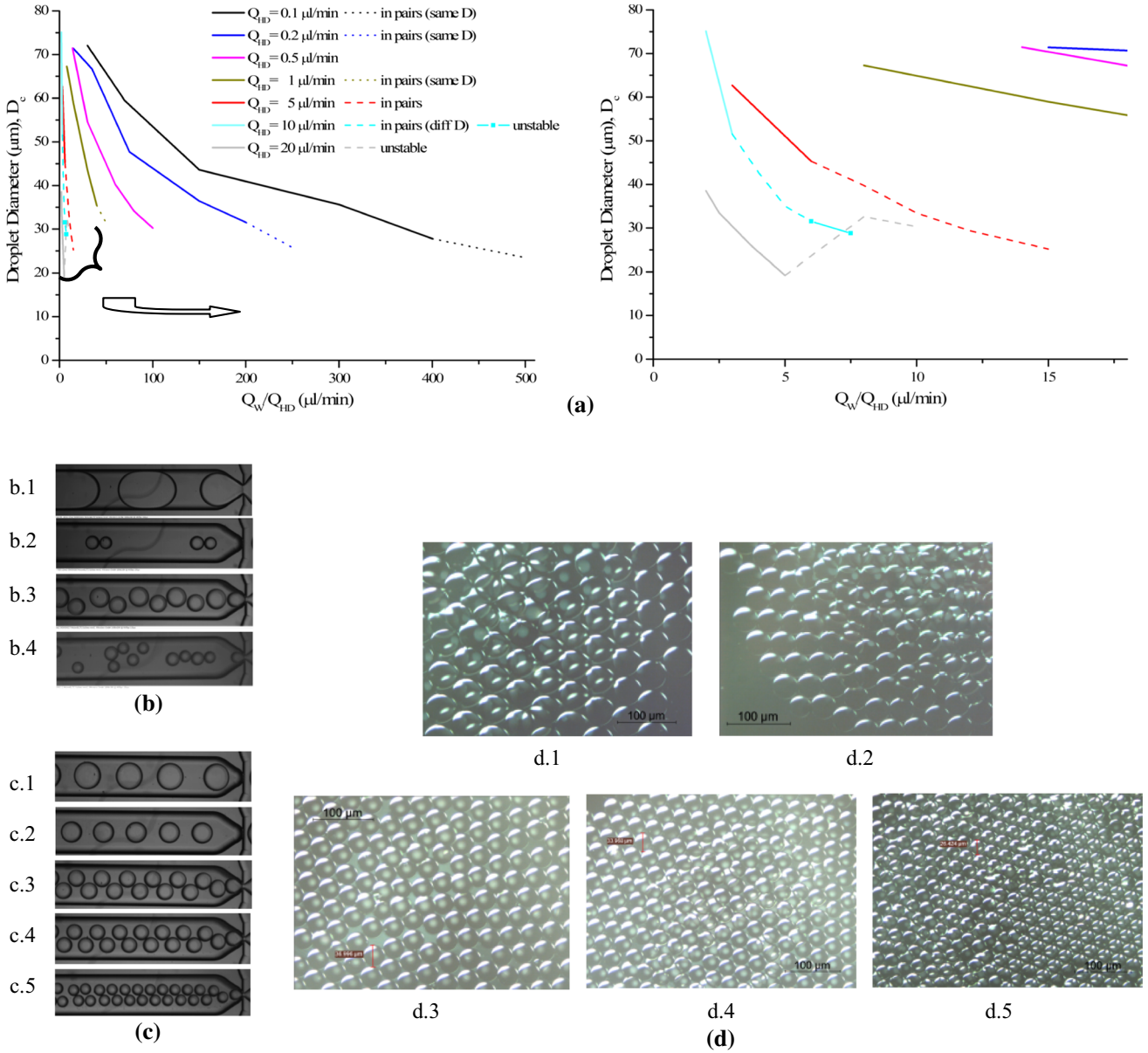

Fig. 9 Hexadecane droplet generation in continuous water phase with a flow-focused design at different HD and W flow rates. **a** Different organic flow rates (Q_{HD}) were fixed by a syringe pump while the aqueous phase flow rate (Q_W) was modulated with the LFCS for each Q_{HD}. The generated droplet diameter inside the channel was measured with a high-speed camera and plotted against flow rate ratio Q_W/Q_{HD}. The *solid lines* represent a stable system where single monodisperse droplets are formed (e.g. with $Q_{HD} = 0.5$ µl/min and $Q_W = 7$–50 µl/min), the *dotted lines* refer to a stable system where monodisperse droplets were generated in pairs and with the same diameter (e.g. with $Q_{HD} = 0.1$ and 0.2 µl/min and $Q_W = 50$ µl/min), the dashed lines indicate an unstable system where pairs or more droplets with different diameters were formed (e.g. with $Q_{HD} = 5$ µl/min and $Q_W = 40$–75 µl/min), and the *solid lines* containing symbol show unstable system where droplets were formed in pairs but being one droplet much bigger than the other (e.g. with $Q_{HD} = 10$ µl/min and $Q_W = 100$–150 µl/min); **b** unstable droplet generations (*b.1*) when a too high Q_{HD}/Q_W ratio deals to droplets that merge because of low surface energy, e.g. for Q_{HD} of 5 µl/min and Q_W of 10 µl/min, (*b.2*) when $Q_W \gg Q_{HD}$ droplets are formed in pairs of similar diameter, e.g. for Q_{HD} of 1 µl/min and Q_W of 50 µl/min, and (*b.3*) increasing Q_{HD} the droplets are formed in pairs but with different diameter, e.g. for Q_{HD} of 10 µl/min and Q_W of 50 µl/min, and (*b.4*) when Q_W is further increased and the system turns into unstable, e.g. for Q_{HD} of 10 µl/min and Q_W of 75 µl/min; **c** stable generation of HD droplets inside the channel with a D_c of (*c.1*) 63 µm for $Q_W = 15$ µl/min and $Q_{HD} = 5$ µl/min, (*c.2*) 45 µm for $Q_W = 30$ µl/min and $Q_{HD} = 5$ µl/min, (*c.3*) 38 µm for $Q_W = 40$ µl/min and $Q_{HD} = 20$ µl/min, (*c.4*) 33 µm for $Q_W = 50$ µl/min and $Q_{HD} = 20$ µl/min, and (*c.5*) 25 µm for $Q_W = 75$ µl/min and $Q_{HD} = 20$ µl/min; **d** stable HD droplets collected in a reservoirs showing realistic droplet diameters of (*d.1*) 53 µm for $Q_W = 15$ µl/min and $Q_{HD} = 5$ µl/min, (*d.2*) 40 µm for $Q_W = 30$ µl/min and $Q_{HD} = 5$ µl/min, (*d.3*) 37 µm for $Q_W = 40$ µl/min and $Q_{HD} = 20$ µl/min, (*d.4*) 34 µm for $Q_W = 50$ µl/min and $Q_{HD} = 20$ µl/min, and (*d.5*) 26 µm for $Q_W = 75$ µl/min and $Q_{HD} = 20$ µl/min. Tween80 surfactant has been added to the water phase, 2% (v/v), so as to avoid merging of HD droplets

tend to merge due to their low surface energy compared to the droplet size, Fig. 9b.1, and consequently, no droplets are formed. When Q_W is much higher than Q_{HD}, the droplets tend to form in pairs showing the same or very similar diameter for low Q_{HD} (depicted in Fig. 9a with dotted lines, e.g. for $Q_{HD} = 0.1–1$ µl/min and shown in Fig. 9b.2), but increasing Q_{HD} pairs of droplets with different diameters were achieved being the first droplet larger than the second and consequently losing the monodispersity (depicted in Fig. 9a with dashed lines, e.g. for $Q_{HD} = 5–10$ µl/min and shown in Fig. 9b.3. For sufficiently high Q_{HD} (e.g. 20 µl/min) and Q_W (e.g. 40–100 µl/min), a stable system with a high generating frequency is achieved (Fig. 9c, d) until Q_W is too high and the system becomes unstable (Fig. 9b.4), resulting in droplets with uncontrolled sized and generating frequencies (depicted in Fig. 9a with solid lines with symbol, e.g. for $Q_{HD} = 10$ µl/min and shown in Fig. 9b.4).

Overall, an increase in flow rates of both phases increases droplet generation frequency. Increasing Q_W for a fixed Q_{HD} leads to a decrease in the droplet diameter, and on the contrary, increasing Q_{HD} for a fixed Q_W increases the droplet diameter. Finally, a stable system is obtained for high Q_{HD} (higher than 5 µl/min) until the aqueous phase flow rate is approximately five times higher than that of the organic phase ($Q_W/Q_{HD} = 5$), after which monodispersity of droplet diameter is lost.

5 Conclusions

The LFCS device presented in this work demonstrates a lean and defect-free manufacturing process for integration of distinct components that are previously designed and optimized as modular approaches, evidencing that the integrated whole device maintains a successful performance as the single modules. Therefore, the method is a realistic option for high-quality prototyping of diverse microfluidic elements in a final polymeric material, reducing the risks and costs associated with LoC optimization for mass production, and being compatible with roll-to-roll, injection moulding, thermocompression, inkjet printing and other techniques commonly found in industrial manufacturing. Moreover, any other microfluidic modules (channels, chambers, mixers, sensors, valves, etc.) can be optimized in single modules and easily included in the final prototypes due to the integrability of the fabrication process, which enhances the integration of many microfluidic systems in other fields, such as biology, pharmacy or chemistry, e.g. microreactors for cell culture, integrated sensing and optical systems for analytical systems.

The LFCS, entirely manufactured in COP polymer, integrates a pneumatic microvalve and a thermal microflow sensor with a bypass structure that have been previously designed and optimized as modular approaches (Etxebarria et al. 2014, 2016). The characterization results for the LFCS demonstrate an excellent performance of the device, since the delivery of the flow rates between 30 and 230 µl/min perfectly matches the flow values defined by the user as well as the commercial flow sensor readouts with an error of less than 5%, indicating that accurate automatic flow controlling concept can be achieved in a low-cost and disposable device. The validation of the LFCS in a high-throughput hexadecane droplet formation confirms the excellent performance of the system, showing high accuracy and reproducibility in autonomous flow regulation that leads to a stable system for the continuous water phase and thus successful monodisperse droplet generation for a wide flow range.

The device offers immense potential for a great amount of research applications dealing with stable and pulseless flows, but it can also be used to generate pulsed periodic flows due to the fast response of the system by defining periodic pressure drop routines. As it is demonstrated in a previous work that presents solely the flow sensor module included in this system (Etxebarria et al. 2016), the fabrication method and performance make it compatible with biological applications and sensitive environments such as cell culture. Accordingly, the previous work can be further extended by using the LFCS to adjust the flow rate variation due to cell growth, inducing a controlled shear stress to cells at every moment. Therefore, the LFCS can be used to modulate and control the fluidic microenvironment in cell applications, to act upon cells by changing the perfusion mode or to easily change medium and nutrients concentrations in droplets that encapsulate cells.

Acknowledgements This work has been funded by the microSCALE ETORTEK Programme of the Basque Government. The authors would like to acknowledge Mikel Gómez, Javier Aduaga and Javier Besteiro from *IK4-IKERLAN S. Coop.* and Dr. Roald Tiggelaar from *MESA+ Institute for nanotechnology* for technical support.

References

Bertholle F, Velvé Casquillas G Digital microfluidics using pressure driven flow [Online]. Available: http://www.elveflow.com/microfluidic/Microfluidic%20droplets%20with%20elveflow%20pressure%20driven%20flow.pdf

Choi JW, Kang DK, Park H, deMello AJ, Chang SI (2012) High-throughput analysis of protein-protein interactions in picoliter-volume droplets using fluorescence polarization (in eng). Anal Chem 84(8):3849–3854

Etxebarria Elezgarai J (2015) Modular integration and on-chip sensing approaches for tunable fluid control polymer microdevices. Ph.D., Chemical Engineering and Environmental Engineering, UPV/EHU University of Basque Country

Etxebarria J, Berganzo J, Elizalde J, Fernandez LJ, Ezkerra A (2014) Highly integrated COP monolithic membrane microvalves by robusthot embossing. Sens Actuators B Chem 190:451–458

Etxebarria J, Berganzo J, Elizalde J, Llamazares G, Fernandez LJ, Ezkerra A (2016) Low cost polymeric on-chip flow sensor with nanoliter resolution. Sens Actuators B Chem 235:188–196

Kohl M, Liu Y, Dittmann D (2004) A polymer-based microfluidic controller. In: 17th IEEE Internat. Conf. on micro electro mechanical systems, Maastricht, NL, Technical Digest New York, N.Y, 25–29 Jan 2004

Lammerink TSJ, Elwenspoek M, Fluitman JHJ (1993) Integrated micro-liquid dosing system. In: Proceedings of IEEE-MEMS workshop, pp 254–9

Pollack MG, Shenderov AD, Fair RB (2002) Electrowetting-based actuation of droplets for integrated microfluidics. Lab Chip 2:96–101

Teh SY, Lin R, Hung LH, Lee AP (2008) Droplet microfluidics. Lab Chip 8:198–220

Utada AS, Lorenceau E, Link DR, Kaplan PD, Stone HA, Weitz DA (2005) Monodisperse double emulsions generated from a microcapillary device. Science 308:537–541

Xie J, Shih J, Tai YC (2003) Integrated surface-micromachined mass flow controller. In: IEEE sixteenth annual international conference on micro electro mechanical systems

Xu W, Wu LL, Zhang Y, Xue H, Li GP, Bachman M (2010) A vapor based microfluidic flow regulator. Sens Actuators B Chem 142:355–361

Zeng W, Li S, Wang Z (2015) Characterization of syringe-pump-driven versus pressure-driven microfluidic flows. Presented at the international conference on fluid power and mechatronics